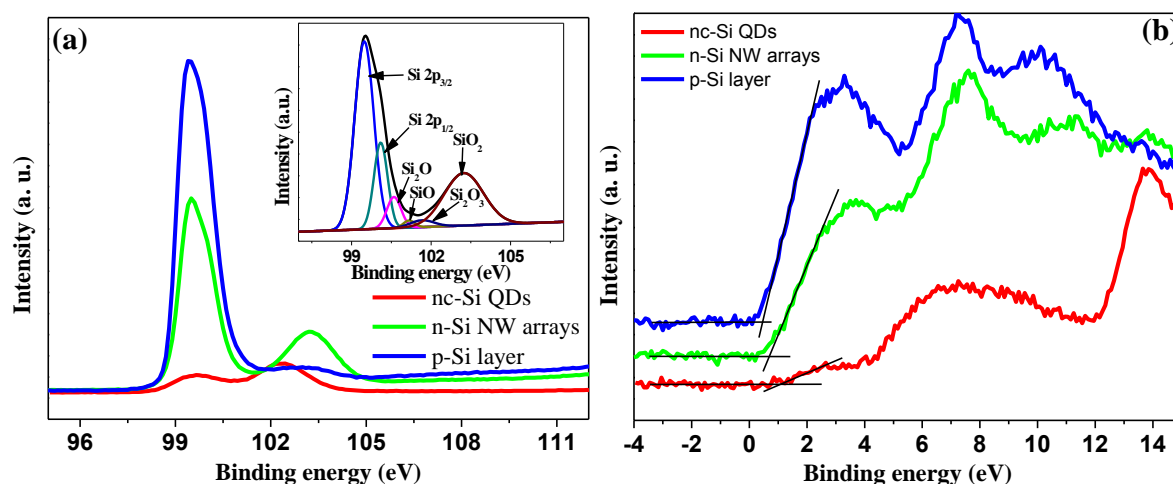


# High Efficiency Hybrid Solar Cells Using Nanocrystalline Si Quantum Dots and Si Nanowires

Mrinal Dutta\*, Lavanya Thirugnanam, Pham Van Trinh and Naoki Fukata\*

International Center for Materials Nanoarchitectonics (MANA), National Institute for Materials Science, 1-1 Namiki, Tsukuba, 305-0044, Japan

## Supporting information



**Figure S1.** (a) High resolution Si 2p and (b) valence band XPS spectrum of nc-Si QDs, n-Si NW arrays and p-Si layer.

Figure S1a shows the Si 2p XPS spectrum of the components of the hybrid solar cell. All the spectra show the presence of two peaks: one assigned to the metallic Si  $2p^{3/2}$  of silicon and another  $Si^{4+} 2p^{3/2}$  of sub oxides on the surface [1]. Deconvolution of the Si 2p spectrum reveals the presence of  $Si_2O$ ,  $SiO$ ,  $Si_2O_3$  or rather more specifically intermediate oxidation states  $Si^{1+}$ ,  $Si^{2+}$ ,  $Si^{3+}$  (inset to Figure S1a is a representative deconvoluted spectrum) [2-5]. The presence of an oxide layer on the surface of nc-Si QDs demonstrates the growth of oxide layer on HF-etched Si nanocrystals during capping. Presence of this oxide layer may be a possible cause of the low quantum yield (30%) of these nc-Si QDs. The XPS spectrum of the valence band (VB) shows a sharp rise near 0.69 eV, 0.47 eV and 1.1 eV, associated with the onset of the VB of n-Si nanowire arrays, polycrystalline p-Si film and nc-Si QDs, respectively. The VB maximum positions are determined by a linear extrapolation of the leading edge of the photoelectron valence-band spectrum back to the energy axis. Defining the slope intercept as the VBM is widely used to determine the VBM of semiconductors to an accuracy of about 0.1 eV [6, 7]. From the above measurements, the valence band offset ( $\Delta E_v$ ) value in the interface between the p-Si layer and nc-Si QDs can be estimated to be  $\sim 0.63$  eV. Using this  $\Delta E_v$  conduction band offset can be estimated using

$$\Delta E_c = \Delta E_v + E_g^{\text{p-Si}} - E_g^{\text{nc-Si}}$$

where  $E_g^{\text{nc-Si}}$  and  $E_g^{\text{p-Si}}$  are the band gap of nc-Si QDs and p-Si layer respectively. Assuming the bandgap of p-Si layer to be close to that of bulk Si,  $\Delta E_c$  can be estimated as ~0.23 eV. Thus, this measurement indicates type I band alignment in the interface of the p-Si layer and nc-Si QDs, as shown in Figure S2 (ignoring the presence of SiO<sub>2</sub> for simplicity).

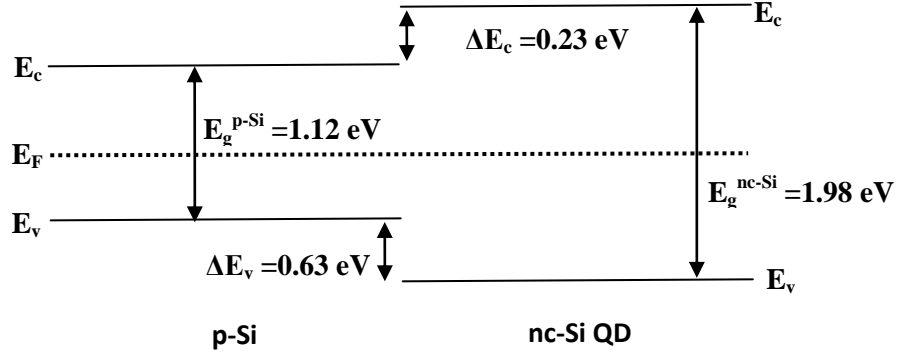


**Figure S2.** Band alignment at the interface of p-Si layer and nc-Si QDs

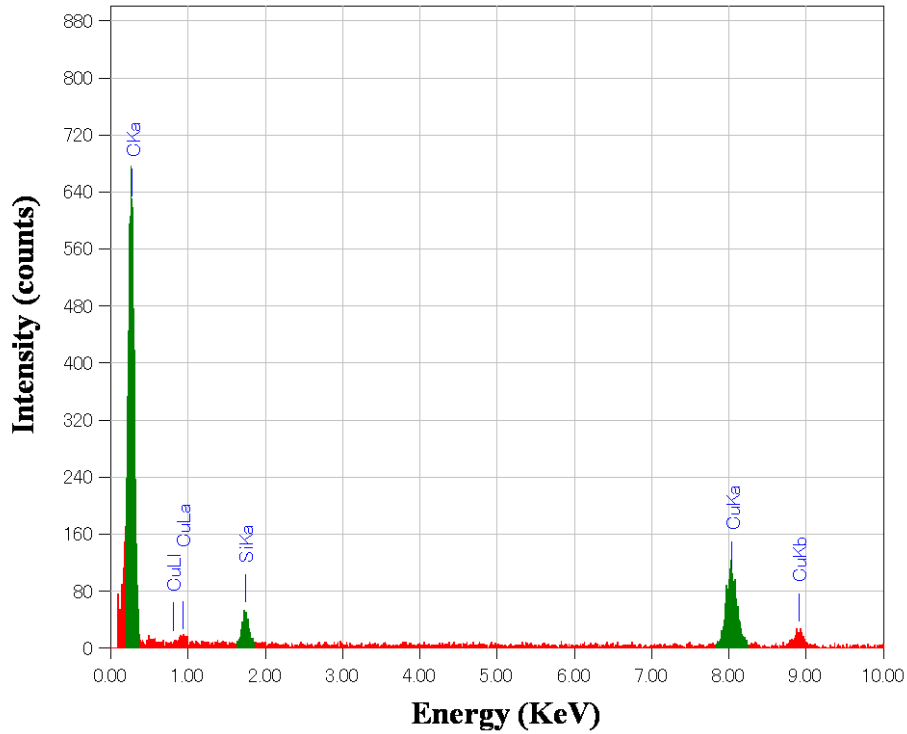


**Figure 3.** EDS spectrum of nc-Si QDs

The composition of the nc-Si QDs was confirmed by energy dispersive X-ray (EDX) spectroscopy (Figure S3), demonstrating that samples consist of Si. However no traces of O

element was detected in comparison with XPS measurement [Figure S1 (a)] because XPS is a surface sensitive technique and XPS measurements suggest very low amount of oxides that may be lower than the detection level of EDX measurement. The C peak arises from the surface bonded alkyl groups and the holey carbon films on a TEM grid. They cannot be differentiated. Cu peaks are due to the TEM grid of Cu.

1. Hessel, C. M.; Henderson, E. J.; Veinot, J. G. C. Hydrogen Silsesquioxane: A Molecular Precursor for Nanocrystalline Si-SiO<sub>2</sub> Composites and Freestanding Hydride-Surface-Terminated Silicon Nanoparticles. *Chem. Mater.* **2006**, 18, 6139-6146.
2. Bashouti, M. Y.; Sardashti, K.; Risteinb J.; Christiansen, S. H. Early Stages of Oxide Growth in H-Terminated Silicon Nanowires: Determination of Kinetic Behavior and Activation Energy. *Phys. Chem. Chem. Phys.*, **2012**, 14, 11877–11881.
3. Himpsel, F. J.; McFeely, F. R.; Taleb-Ibrahimi, A.; Yarmoff, J. A.; Hollinger, G. Microscopic Structure of the SiO<sub>2</sub>/Si Interface, *Phys. Rev. B* **1988**, 38, 6084-6096.
4. Thgersen, A.; Josefine, S. H.; Marstein, E. S. Oxidation Effects on Graded Porous Silicon Anti-Reflection Coatings. *J. Electrochem. Soc.* **2012**, 159, D276-D28.
5. Purkait, T. K.; Iqbal, M.; Wahl, M. H.; Gottschling, K.; Gonzalez, C. M.; Islam, M. A.; Veinot, J. G. C. Borane-Catalyzed Room-Temperature Hydrosilylation of Alkenes/Alkynes on Silicon Nanocrystal Surfaces. *J. Am. Chem. Soc.* **2014**, 136, 17914–17917.
6. Eastman, D. E.; Grobman, W. D.; Freeouf, J. L.; Erbudak, M. Photoemission Spectroscopy Using Synchrotron Radiation. I. Overviews of Valence-Band Structure for Ge, GaAs, GaP, InSb, Znse, CdTe, and Agl. *Phys. Rev. B* **1974**, 9, 3473-3488.
7. Kraut, E. A.; Grant, R. W.; Waldrop J. R.; Kowalczyk S. P. Semiconductor Core-Level to Valence-Band Maximum Binding-Energy Differences: Precise Determination by X-Ray Photoelectron Spectroscopy. *Phys. Rev. B* **1983**, 9, 1965-1976.